A LETTERS JOURNAL EXPLORING
THE FRONTIERS OF PHYSICS

OFFPRINT

Water at the cavitation limit: Density of the metastable liquid and size of the critical bubble

KRISTINA DAVITT, ARNAUD ARVENGAS and FRÉDÉRIC CAUPIN

EPL, **90** (2010) 16002

Please visit the new website
www.epljournal.org

TARGET YOUR RESEARCH WITH EPL

Sign up to receive the free EPL table of contents alert.

www.epljournal.org/alerts

A Letters Journal Exploring the Frontiers of Physics

April 2010

EPL, **90** (2010) 16002
doi: 10.1209/0295-5075/90/16002

www.epljournal.org

Water at the cavitation limit: Density of the metastable liquid and size of the critical bubble

Kristina Davitt, Arnaud Arvengas and Frédéric Caupin[(a)]

Laboratoire de Physique Statistique, Ecole Normale Supérieure, UPMC Université Paris 06, Université Paris Diderot, CNRS - 24 rue Lhomond, 75005 Paris, France, EU

received 26 January 2010; accepted in final form 18 March 2010
published online 27 April 2010

PACS 64.60.qj – Studies of nucleation in specific substances
PACS 64.70.F- – Liquid-vapor transitions
PACS 82.60.Nh – Thermodynamics of nucleation

Abstract – The ability of a liquid to sustain mechanical tension is a spectacular manifestation of the cohesion of matter. Water is a paradigmatic example, because of its high cohesion due to hydrogen bonds. The knowledge of its limit of rupture by cavitation can bring valuable information about its structure. Up to now, this limit has been obscured by the diversity of experimental results based on different physical measures of the degree of metastability of the liquid. We have built a fiber optic probe hydrophone to provide the missing data on the density of the liquid at the acoustic cavitation limit. Our measurements between 0 and 50 °C allow a clear-cut comparison with another successful method where tension is produced in micron-sized inclusions of water in quartz. We also extend previous acoustic measurements of the limiting pressure to 190 °C, and we consider a simple modification of classical nucleation theory to describe our data. Applying the nucleation theorem gives the first experimental value for the size of the critical bubble, which lies in the nanometer range. The results suggest the existence of either a stabilizing impurity in the inclusion experiments, or an ubiquitous impurity essential to the physics of water.

Copyright © EPLA, 2010

Introduction. – The behavior of liquid water under mechanical tension is relevant to topics as diverse as sap flow in trees [1,2], efficiency of cephalapod suckers [3], or microfluidic tension pumps and heat sinks [4]. The existence of this metastable state has been observed since the time of Huygens [5], and has since been the subject of numerous experimental investigations [6]. However, there is no consensus on the measured cavitation limit —that at which the metastable liquid "breaks" by nucleation of vapor bubbles. The cavitation limit has many practical implications, and it is also of fundamental interest in understanding the numerous anomalies of water, such as the well-known fact that the liquid expands when it is cooled below 4 °C. Several reviews have delineated the scenarios proposed to explain these anomalies [7–11].

Let us first recall the origin of the ability of a liquid to sustain tension. As its pressure is decreased, a liquid should begin to boil when it reaches the saturated vapor pressure, at which the chemical potentials of the liquid and vapor are equal. However, the liquid-vapor interface which needs to be created for a bubble to form has a cost due to surface energy. Therefore, the nucleation of vapor can be delayed: the liquid is then metastable, and can even reach negative pressures. The competition between volume and surface energy results in an energy barrier E_b which decreases when the pressure becomes more negative, until the barrier is sufficiently low to be overcome by thermal fluctuations of the system. This is the basis of nucleation theory, which predicts that liquid water can reach pressures beyond −120 MPa at room temperature [12]. This large negative value comes from the high surface energy, a signature of the strong cohesion of water.

We will first review some experiments on cavitation in water. We emphasize the difficulty inherent in their comparison, due to their use of different physical measures of metastability. We will then describe a direct measurement of the density of liquid water at the cavitation limit in an acoustic experiment. This allows an unambiguous comparison with the cavitation density determined by another method, based on micron-sized inclusions of water in quartz. We find a large discrepancy at room temperature. This led us to extend the acoustic measurements up to 190 °C, where our data overlap with some of the inclusion results. We then compare our data

[(a)] E-mail: caupin@lps.ens.fr

with theory and analyze them to calculate the volume of water involved in the nucleation process. Finally, we discuss possible explanations for the discrepancy between experiments.

Previous studies. – An extensive review of cavitation in water can be found in ref. [6]. Here we only summarize the three methods that were able to reach a large degree of metastability over a wide temperature range. Briggs used the centrifugation method [13], which consists in spinning a tube full of liquid perpendicularly to its axis. At the center of rotation, the centrifugal force exerts a tension on the liquid, $P = P_0 - \frac{1}{2}\rho\omega^2 r^2$, where P_0 is the pressure outside the tube, ρ is the water density, and r is the distance between the center and the liquid-gas interface. The cavitation pressure P_{cav} obtained by Briggs exhibits a minimum of $-27.7\,\mathrm{MPa}$ at $10\,^\circ\mathrm{C}$, with $P_{\mathrm{cav}} = -2\,\mathrm{MPa}$ at $0\,^\circ\mathrm{C}$ and $-22\,\mathrm{MPa}$ at $50\,^\circ\mathrm{C}$. Note that, as is often the case, the values reported are the largest tension achieved and that cavitation usually occured before.

Another way to generate tension is to use a piezoelectric transducer to generate an acoustic wave, which successively pressurizes and stretches the liquid. Cavitation occurs at large enough amplitudes. We estimated P_{cav} in an acoustic experiment by two methods [14]. The first relies on a commercial piezoelectric hydrophone. The second uses the static pressure method (SPM). It consists in measuring the relation between the transducer voltage required for cavitation, V_{cav}, and the ambient static pressure in the liquid, P_{stat}. The relation between V_{cav} and P_{stat} is linear in the range 1–10 MPa, and can be extrapolated down to zero voltage to get an upper bound on P_{cav} [14]. The two methods agree and yield P_{cav} varying from $-26\,\mathrm{MPa}$ at $0\,^\circ\mathrm{C}$ to $-17\,\mathrm{MPa}$ at $80\,^\circ\mathrm{C}$. This matches the values obtained by centrifugation above $10\,^\circ\mathrm{C}$ [13], and also those obtained with various other methods over a reduced temperature range [4,6].

Experiments on microscopic quartz inclusions [15,16] seem to be the only ones able to reach a higher degree of metastability: the largest P_{cav} was estimated to be $-140\,\mathrm{MPa}$, which is compatible with theoretical predictions. However, there is some uncertainty in this pressure estimate, as can be understood from the details of the method. Small sealed cavities (in the 10–100 μm range) filled with water are prepared in a quartz crystal. Any vapor bubble present shrinks upon heating along the line of liquid-vapor equilibrium. The bubble eventually disappears at a temperature from which the liquid density is deduced. Then, when the inclusion is cooled down, the bubble does not reappear immediately. Assuming that the inclusion volume and the amount of water remain constant, the liquid is brought in the negative pressure region following an isochore, until cavitation occurs. To estimate P_{cav} from the measured density, one must rely on an equation of state (EoS), which is extrapolated from data measured in the positive pressure range (*e.g.* [17]). As the largest tension reported is $-144\,\mathrm{MPa}$ at $40\,^\circ\mathrm{C}$ [15], the extrapolation involved can be quite long. In addition, this large value was only obtained in one sample, and the data show considerable scatter. The overall results of this work have been reproduced [18,19].

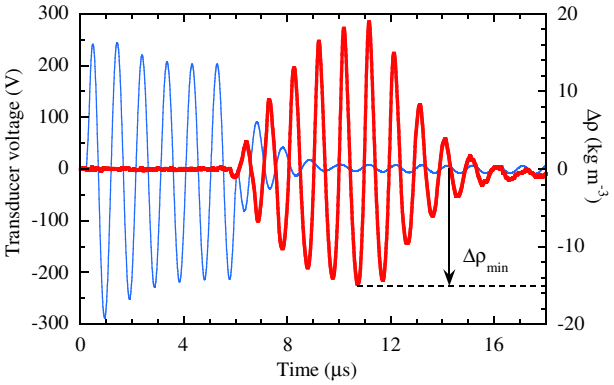

Fig. 1: (Color online) Excitation voltage on the transducer (thin blue line, left axis) and resulting density change (thick red line, right axis) measured at $1\,^\circ\mathrm{C}$ and $0.83\,V_{\mathrm{cav}}$. The optical signal is averaged over 100 bursts to the transducer.

There is a discrepancy between the pressures reported for cavitation with the centrifugal and acoustic methods on the one hand, and with the inclusion method on the other hand. However, the comparison is complicated by the use of an extrapolated EoS. Thus, the discrepancy may only be apparent. This is what led us to devise a method to directly measure the density of water stretched to the cavitation limit by an acoustic wave.

Experimental setup. – We use a piezoelectric transducer driven in bursts of 6 cycles at its resonance frequency of 1.03 MHz with a repetition rate of 1.75 Hz (fig. 1). We have previously described this method in detail [14]. Its main advantage is that focusing of the acoustic wave enables the study of a small volume of water over a short period of time and far away from any wall, thus reducing the influence of heterogeneous cavitation nuclei: a high nucleation rate is achieved, around $10^{11}\,\mathrm{mm^{-3}\,s^{-1}}$. Cavitation bubbles are detected from the echo of the acoustic wave reflected by the bubble surface back to the transducer. The high stability of the setup allows us to repeat the bursts under the same experimental conditions, demonstrating the stochastic nature of cavitation. Its probability, Σ, changes from 0 to 1 in a narrow range of values of the excitation voltage, V. We define the cavitation voltage, V_{cav}, as the value at which $\Sigma = 1/2$. The plot of Σ *vs.* V, which we call an S-curve, has a characteristic double exponential shape, reflecting the thermally driven nature of cavitation [14]. The transducer is immersed in ultrapure water in an open Pyrex glass container. Our previous studies, which included measurements on degassed water transferred under vacuum in a sealed experimental cell [14], and water saturated with various gases [20], have shown that the technique is not sensitive to gas content.

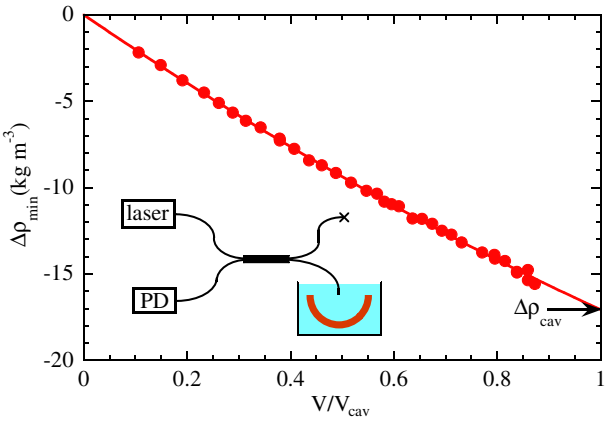

Fig. 2: (Color online) Density change at the acoustic wave minimum as a function of $V/V_{\rm cav}$ at 1 °C. The solid line is a parabolic fit to the data where $V/V_{\rm cav} \leqslant 0.6$; data at higher fractions of $V_{\rm cav}$ illustrate that the extrapolation holds. The inset shows a sketch of the apparatus.

To measure the density of water during the application of an acoustic burst, we have built a fiber optic probe hydrophone (FOPH) [21] (fig. 2). It uses a step index fiber (core/clad of 50/125 μm) with a pure silica core of index $n_{\rm f}$. A laser beam is directed through a 2×2 fiber coupler to a bare fiber tip immersed in the liquid. The reflection coefficient of the fiber-liquid interface,

$$R\,(t) = \left(\frac{n(t) - n_{\rm f}}{n(t) + n_{\rm f}}\right)^2, \qquad (1)$$

is measured with a photodiode (PD) located on the other input of the coupler to obtain $n(t)$, the index of water at the fiber tip, modulated in time by the acoustic wave. The modulation of the reflected light intensity is small, therefore we use an average over 100 bursts at each voltage to improve the signal-to-noise. Finally, the index is converted into density using the IAPWS formulation [22]. Figure 1 shows the drive applied to the transducer and the resulting change in density, $\Delta\rho$, occurring after a delay corresponding to the time-of-flight of the ultrasonic wave. At each temperature the excitation voltage is ramped from 0.1 to 0.6 $V_{\rm cav}$. An S-curve is measured before and after each ramp. The drift in $V_{\rm cav}$ is always less than 5%, and the average is used in the analysis.

Cavitation density. – The density change at the focus and at the acoustic wave minimum, $\Delta\rho_{\rm min}$, is plotted as a function of $V/V_{\rm cav}$ (fig. 2). We note that the variation is slightly less than linear (see below). We have extrapolated the data below 0.6 $V_{\rm cav}$ with a parabola up to $V_{\rm cav}$. We have checked at 1 (fig. 2), 12, 20, and 47 °C that this extrapolation reproduces correctly the data up to 0.9 $V_{\rm cav}$. For other temperatures, the ramp was limited to below 0.6 $V_{\rm cav}$ to avoid cavitation on the fiber tip. Repeated checks of the data at 20 °C were performed to ensure that no damage occurred, otherwise the fiber was re-cleaved.

The cavitation densities, $\rho_{\rm cav}$, determined from extrapolations of the parabolic fit are shown in fig. 3. Note

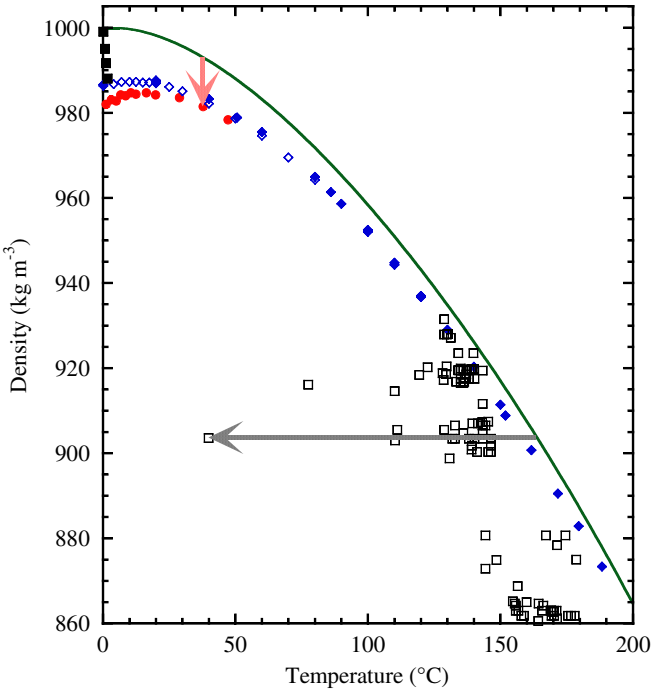

Fig. 3: (Color online) Cavitation density as a function of temperature. The green curve gives the density of water at saturated vapor pressure. In the acoustic experiment, water is streched along an isentropic (quasi-isothermal [14]) path, illustrated by the vertical arrow. $\rho_{\rm cav}$ is obtained by direct FOPH measurements (red circles) and by converting into density $P_{\rm cav}$ estimated with the SPM (blue open [14] and filled (this work) diamonds). Statistical errors are smaller than the symbol size. In the inclusion experiment [16], water follows an isochoric path, illustrated by the horizontal arrow, until it cavitates (open black squares). Cavitation also occurs in inclusions heated along the metastable ice-liquid equilibrium (filled black squares).

that we have repeated the procedure with acoustic bursts at 2 MHz and obtained the same $\rho_{\rm cav}$ (not shown) within the error bars. We can now compare our results directly with the inclusion work. The discrepancy is obvious (fig. 3). For inclusions in a high-density sample ($900.3 \leqslant \rho \leqslant 907.4\,{\rm kg\,m^{-3}}$), cavitation temperatures ranged from 39.9 to 143.3 °C [16]. This shows considerable scatter in the data, but is nonetheless markedly different from our results at comparable temperatures. For example, at 39.9 °C, $\rho_{\rm cav} = 903.6\,{\rm kg\,m^{-3}}$ was reported [16], much lower than the present 981 kg m^{-3}. As the density is the measured quantity in both experiments, the discrepancy we find is independent of any assumption on the EoS. However, because of the extreme reproducibility of the acoustic method [14], this discrepancy is surprising, and one wonders if it arises from a fundamental phenomenon. For instance, as the two experiments follow different paths in the phase diagram (see arrows in fig. 3), a path-dependent nucleation mechanism might be involved. To clarify this issue, we decided to extend the acoustic measurements to higher temperatures.

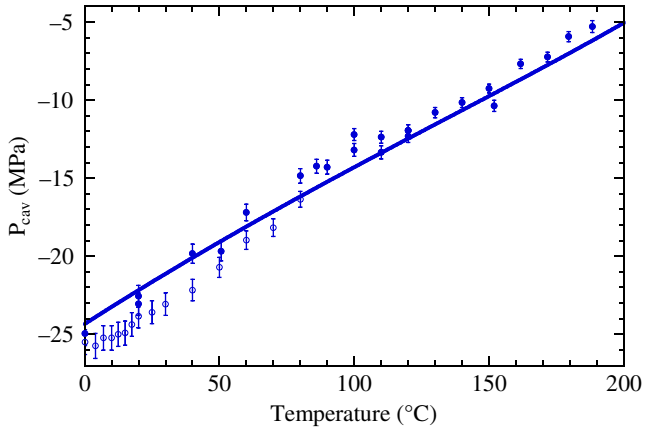

Fig. 4: (Color online) Acoustic cavitation pressure as a function of temperature. The open [14] and filled (this work) circles show the values obtained with the SPM. The curve shows the CNT prediction, using a rescaled surface tension, $\sigma_{\rm eff} = 0.237\,\sigma_{\rm bulk}$.

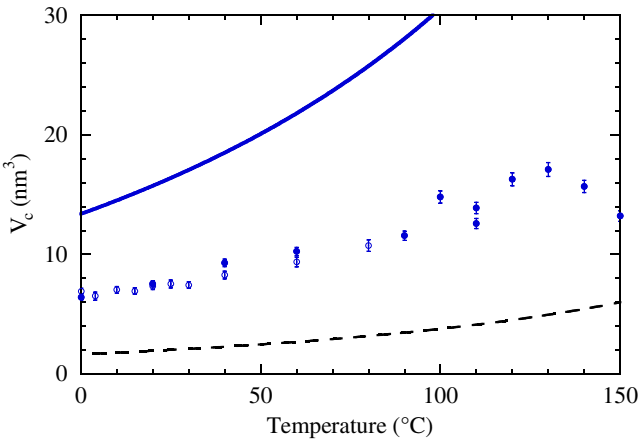

Fig. 5: (Color online) Volume of the critical bubble as a function of temperature. The open [14] and filled (this work) circles show the value deduced from the cavitation statistics with the nucleation theorem. The dashed and solid curves show the CNT prediction, using the bulk surface tension of water and a rescaled value ($\sigma_{\rm eff} = 0.237\,\sigma_{\rm bulk}$), respectively.

High-temperature results. – In order to access the acoustic focus, density measurements with the FOPH are performed in an open container, which can be used only below 50 °C. To investigate higher temperatures, we returned to a closed high-pressure cell and the SPM. We thereby extended the acoustic data for $P_{\rm cav}$ up to 190 °C, as shown in fig. 4. We convert to $\rho_{\rm cav}$ using an extrapolated EoS [17]. The result displayed in fig. 3 shows that $\rho_{\rm cav}$ converted from SPM values agree with the direct FOPH measurements. We note that the former are systematically slightly larger than the latter; this might arise from the extrapolated EoS or from non-linearities in the focusing of the sound wave, as observed in fig. 2, which would affect the estimate of $P_{\rm cav}$ [14]. Regardless, the difference is much less than the one with the inclusion results, and becomes smaller as the temperature increases. This probably stems from the lower penetration in the metastable region achievable at higher temperature. We can thus rely on the SPM above 50 °C, where direct FOPH measurements are not available. We find that, above 130 °C, the acoustic data merge with the inclusion results showing the least metastability (fig. 3). This means that the thermodynamic path followed by inclusions showing larger metastability (*e.g.* the sample able to reach 40 °C) crosses the path followed by water in the acoustic method. This excludes the possibility that the discrepancy between experiments is due to path-dependent nucleation.

Comparison with theory. – Classical nucleation theory (CNT) describes the nucleation of a spherical vapor bubble separated from the liquid at pressure P by a sharp interface [6]. The critical radius is $R_{\rm c} = 2\sigma/(P_{\rm sat} - P)$, where σ is the surface tension and $P_{\rm sat}$ the saturated vapor pressure. The nucleation rate is $\Gamma = \Gamma_0\, V \tau \exp[-E_{\rm b}/(k_{\rm B}T)]$, where

$$E_{\rm b} = \frac{16\pi}{3}\frac{\sigma^3}{(P_{\rm sat} - P)^2}. \qquad (2)$$

Our definition of $P_{\rm cav}$ from the S-curve corresponds to $\Gamma = \ln 2$, which we solve using the values of the prefactor Γ_0 and of the experimental volume V and time τ given in ref. [14] (see in particular table I). This choice is not critical, since $P_{\rm cav}$ depends only logarithmically on these parameters. The bulk surface tension of water $\sigma_{\rm bulk}$ [22] gives $P_{\rm cav}$ much more negative than in our experiment [6]. However, at each temperature, one can fit the experimental $P_{\rm cav}$ by adjusting σ in eq. (2). Remarkably, this procedure yields an effective surface tension $\sigma_{\rm eff}$ whose ratio to $\sigma_{\rm bulk}$ is nearly constant over the whole temperature range (0.237 average, 0.012 standard deviation). Figure 4 shows how well a simple modification of CNT with a constant $\sigma_{\rm eff}/\sigma_{\rm bulk}$ reproduces our data for $P_{\rm cav}$. We now investigate if the cavitation statistics can also be accounted for with this rescaled $\sigma_{\rm eff}$.

Size of the critical bubble. – The nucleation theorem [23] states that the number of molecules $\Delta n_{\rm c}$ that need to be removed to form the critical bubble is equal to $(\partial E_{\rm b}/\partial \mu_{\rm L})_T$, where $\mu_{\rm L}$ is the chemical potential of the liquid. This relation is model independent, and holds even if $E_{\rm b}$ is different from eq. (2). Our accurate cavitation statistics, combined with the pressure calibration, give us $(\partial E_{\rm b}/\partial P_{\rm L})_T$ (eq. (13) of [14]). Let $v_{\rm L}$ be the volume per molecule in the liquid. We have

$$\left(\frac{\partial E_{\rm b}}{\partial P_{\rm L}}\right)_T = \left(\frac{\partial \mu_{\rm L}}{\partial P_{\rm L}}\right)_T \left(\frac{\partial E_{\rm b}}{\partial \mu_{\rm L}}\right)_T = v_{\rm L}\,\Delta n_{\rm c}, \qquad (3)$$

which is the volume $V_{\rm c}$ that the molecules involved in the critical bubble would occupy in the liquid. Thus, our macroscopic measurement gives access to a microscopic information: the size of the critical bubble. Figure 5 compares the experimental values with the prediction of CNT, $V_{\rm c} = 4\pi R_{\rm c}^3/3$, with $\sigma_{\rm bulk}$ and $\sigma_{\rm eff}$. No choice of σ is able to simultaneously account for our $P_{\rm cav}$ and $V_{\rm c}$

data. Another modification is required. For instance, to reduce V_c, the CNT bubble could be filled with a fluid at a density intermediate between those of the liquid and the vapor. Rather than CNT, more elaborate nucleation theories, such as density functional theory [12], may be needed. Another possibility is an impurity scenario (see below), where the impurity would provide a simultaneous reduction of the energy barrier and of the critical volume. For comparison, it would be interesting to know V_c for the inclusions, but it is not possible with the available data. Simulations are called for to provide more insight.

Discussion. – The discrepancy between acoustic and inclusion experiments remains to be explained. This section proposes some speculative ideas. Before proceeding, let us exclude two reasons sometimes invoked. One might think that the acoustic experiment quenches the liquid too rapidly compared to the inclusion method. However, the acoustic tension lasts around 50 ns, much longer than microscopic relaxation times. There is a dependence of P_{cav} on the experimental time, but it is logarithmic, and has the opposite effect than required to explain the discrepancy: P_{cav} is more negative for a shorter time [14]. Furthermore, other experiments (*e.g.* with the centrifugal [13] or artificial tree [4] methods) have timescales comparable to the inclusion method, but still reach values of P_{cav} close to the acoustic ones. One might also wonder if water in the inclusions is somehow stabilized by a confinement effect from the silica walls. However, any such effect would have a range that is certainly much smaller than the inclusion size (a few microns).

We are therefore left with an explanation involving impurities. There are two possibilities: i) a *stabilizing* impurity that *extends* the achievable range of metastability is present *only in some* of the inclusions; or ii) a *destabilizing* impurity that *reduces* the achievable range of metastability is present in *all* experiments, *except in some* inclusions.

i) *Stabilizing impurities* could be created from the quartz during the fabrication of inclusions, when water reaches supercritical conditions where it is known to dissolve silica. Silica nanoclusters could be formed. However, their effect on cavitation is not clear. They might stabilize the neighboring hydrogen bond network, but this influence is expected to have only a short range, and thus stabilization of the whole sample would require a large cluster concentration, which might be detected by suitable methods.

ii) *Destabilizing impurities* may be present in all experiments, but disappear during the fabrication of inclusions. This could happen thanks to the high pressure and temperatures reached: "surfactant molecules cluster destroyed by annealing at the higher temperatures" have been invoked in [15]. We emphasize that an extremely ubiquitous impurity is required to explain the reproducibility of our cavitation statistics from one water sample to another. For at least one impurity to be present in the volume involved in the acoustic experiment at 2 MHz, the impurity concentration c must exceed $6.3 \times 10^{-14}\,\mathrm{mol\,L^{-1}}$ [14]. On the other hand, in the most metastable inclusions, there should be no impurity in the inclusion volume of around $(10\,\mu\mathrm{m})^3$, requiring $c < 1.7 \times 10^{-12}\,\mathrm{mol\,L^{-1}}$. The overlap between ranges is compatible with the hypothesis that the acoustic experiment is sensitive to impurities whereas the inclusion experiment is not, but the margin is narrow. Another possibility is that the impurities present in bulk water are deactivated by adsorption sites present on the inclusion walls. Assuming $c = 10^{-7}\,\mathrm{mol\,L^{-1}}$ in bulk water, a cubic inclusion with side $a = 10\,\mu\mathrm{m}$ contains 60 impurities, and 1 site per $(100\,\mathrm{nm})^2$ would be needed. $c = 10^{-7}\,\mathrm{mol\,L^{-1}}$ was chosen because hydronium and hydroxide ions are spontaneously created in neutral water ($p\mathrm{H} = 7$) with this concentration by autoprotolysis. This speculation gains support from the fact that inclusions filled with a $1\,\mathrm{mol\,L^{-1}}$ NaOH solution give much less scattered results than with pure water, and on average more negative pressures [19]. Hydronium ions would therefore be good candidates for an ubiquitous impurity, spontaneously present in sufficient quantity in water.

Remaining issues with inclusions. A difficulty with these impurity scenarios is that inclusion experiments exhibit large scatter in the cavitation thresholds for samples with similar densities (fig. 3); therefore, there should be several types of impurities involved, which affect E_b in quantitatively different ways. Furthermore, a fully consistent picture should also explain the surprising behavior of ice-melting in inclusions [16], which has been hitherto overlooked. After an inclusion has been frozen to be filled with ice, the ice melts upon heating. Because of the higher density of the liquid, the system is put under tension, following the metastable liquid-ice equilibrium line, until cavitation occurs. Surprisingly, the largest P_{cav} obtained with this method is −22.8 MPa [16] (fig. 3, lowest filled black square), in an inclusion which cavitated at −103.7 MPa with the usual isochoric liquid cooling method [16][1]. The only change is the presence of the liquid-ice interface. In case i), it would force the stabilizing impurities to disappear or lose their efficiency, by being incorporated in ice or deactivated at its surface, but the mechanism remains unclear. In case ii), ice would trigger heterogeneous nucleation. With CNT, this can occur due to incomplete wetting of a substrate [6]. However, a reduction of P_{cav} by a factor of 4.5, as observed in one of the inclusions, would require a contact angle of the liquid on ice of 113°, far above the observed 1° [25].

[1] We note that ice-liquid equilibrium was observed up to 6.5 °C in natural-fluorite inclusions [24]. However, this work involved aqueous solutions of unknown composition and contained no corresponding study of high-temperature cavitation.

A microscopic interpretation is needed: ice being less dense than the liquid, the interface might provide heterogeneous nucleation sites facilitating the formation of vapor.

Path-dependent nucleation. We have mentioned above a nucleation mechanism depending on the thermodynamic path followed in the phase diagram to stretch water. We have seen that the discrepancy between the acoustic and inclusion experiments cannot be explained by such a mechanism, because our high-temperature experiments cross the path followed by the inclusions. Nevertheless, this scenario might be invoked to explain the behavior of ice-melting in inclusions just mentioned. What could be the microscopic origin of such a path-dependent cavitation? Using CNT with $\sigma_{\rm bulk}$ yields $P_{\rm cav}$ values close to those estimated for isochorically cooled inclusions [12,15]. During ice-melting in inclusions, nucleation could occur through an intermediate metastable state which would lower $E_{\rm b}$ because of a lower interfacial tension: this is called the Ostwald step rule, often invoked in crystallization, and recently verified experimentally [26]. This intermediate state could be another liquid phase of water, such as the low-density liquid phase found by all molecular-dynamics simulations [7–11]. However, the first-order transition they predict usually ends with a metastable critical point (MCP) at positive pressure in the supercooled regions. Yet some simulations have also found an MCP at negative pressure [11,27,28]. Analytic models have also shown that a change of parameters could move the MCP to negative pressures and room temperature [29,30]. Furthermore, simulations of a model globular protein have shown how the vicinity of a fluid-fluid MCP in the phase diagram of the protein largely reduces $E_{\rm b}$ for its crystallization [31]. When water in the inclusions is stretched during ice-melting, cavitation could thus be affected by the vicinity of an MCP at negative pressure. On the other hand, the isochoric path usually followed by the inclusions goes through a region of large tension at high temperature. Thus, it may avoid the critical region and yield $P_{\rm cav}$ expected from CNT with $\sigma_{\rm bulk}$. To check the possibility of this mechanism, simulations are clearly needed.

Conclusion. – Using a method with great reproducibility, we have measured the density of liquid water at the acoustic cavitation limit, and obtained the size of the critical bubble through the nucleation theorem. Our results stand in contrast with both theory and one experiment based on inclusions of water in quartz. However, the acoustic cavitation limit at high temperature merges with the inclusions showing the lowest metastability. We have discussed possible explanations to account for these findings; one of them involves the role of hydronium ions, and calls for simulations of cavitation in their presence.

* * *

We thank S. Cersoy, J. Dubail, and R. Sheshka for their participation in early stages of the experiment. Discussions with S. Balibar, G. Franzese and A. D. Stroock are acknowledged. We are particularly indebted to C. A. Angell for his valuable advice and for providing Q. Zheng's thesis. This research has been funded by the ERC under the European Community's FP7 *Grant Agreement* No. 240113.

REFERENCES

[1] Tyree M. T. and Zimmermann M. H., *Xylem Structure and the Ascent of Sap,* 2nd edition (Springer-Verlag, Berlin, Heidelberg, New York) 2002.
[2] Cochard H., *C. R. Physique*, **7** (2006) 1018.
[3] Smith A., *J. Exp. Biol.*, **199** (1996) 949.
[4] Wheeler T. D. and Stroock A. D., *Nature*, **455** (2008) 208.
[5] Kell G. S., *Am. J. Phys.*, **51** (1983) 1038.
[6] Caupin F. and Herbert E., *C. R. Physique*, **7** (2006) 1000.
[7] Debenedetti P. G. and Stanley H. E., *Phys. Today*, **56**, issue No. 6 (2003) 40.
[8] Debenedetti P. G., *J. Phys.: Condens. Matter*, **15** (2003) R1669.
[9] Stanley H. *et al.*, *Eur. Phys. J. ST*, **161** (2008) 1.
[10] Angell C. A., *Science*, **319** (2008) 582.
[11] Brovchenko I. and Oleinikova A., *ChemPhysChem*, **9** (2008) 2660.
[12] Caupin F., *Phys. Rev. E*, **71** (2005) 051605.
[13] Briggs L. J., *J. Appl. Phys.*, **21** (1950) 721.
[14] Herbert E., Balibar S. and Caupin F., *Phys. Rev. E*, **74** (2006) 041603.
[15] Zheng Q. *et al.*, *Science*, **254** (1991) 829.
[16] Zheng Q., PhD Thesis, Arizona State University (1991).
[17] Kestin J. *et al.*, *J. Phys. Chem. Ref. Data*, **13** (1984) 175.
[18] Alvarenga A. D., Grimsditch M. and Bodnar R. J., *J. Chem. Phys.*, **98** (1993) 8392.
[19] Shmulovich K. I. *et al.*, *Geochim. Cosmochim. Acta*, **73** (2009) 2457.
[20] Herbert E., PhD Thesis, Université Paris-Diderot - Paris VII (2006).
[21] Staudenraus J. and Eisenmenger W., *Ultrasonics*, **31** (1993) 267.
[22] The International Association for the Properties of Water and Steam, *Release on the Refractive Index of Ordinary Water Substance as a Function of Wavelength, Temperature and Pressure* (IAPWS) 1997; *Release: "Surface Tension of Ordinary Water Substance"* (IAPWS) 1994.
[23] Oxtoby D. W. and Kashchiev D., *J. Chem. Phys.*, **100** (1994) 7665.
[24] Roedder E., *Science*, **155** (1967) 1413.
[25] Ketcham W. M. and Hobbs P. V., *Philos. Mag.*, **19** (1969) 1161.
[26] Chung S. *et al.*, *Nature Phys.*, **5** (2009) 68.
[27] Brovchenko I., Geiger A. and Oleinikova A., *J. Chem. Phys.*, **123** (2005) 044515.
[28] Tanaka H., *J. Chem. Phys.*, **105** (1996) 5099.
[29] Poole P. *et al.*, *Phys. Rev. Lett.*, **73** (1994) 1632.
[30] Stokely K. *et al.*, *Proc. Natl. Acad. Sci. U.S.A.*, **107** (2010) 1301.
[31] ten Wolde P. R. and Frenkel D., *Phys. Chem. Chem. Phys.*, **1** (1999) 2191.